JOURNAL OF THEORETICAL
AND APPLIED MECHANICS
1, 38, 2000

ESTIMATION OF LOAD CARRYING CAPACITY OF THIN-WALLED COMPOSITE STRUCTURES

ZBIGNIEW KOŁAKOWSKI
MARIAN KRÓLAK
KATARZYNA KOWAL-MICHALSKA
SŁAWOMIR KĘDZIORA

Department of Strength of Materials and Structures, Technical University of Łódź
e-mail: kola@orion.p.lodz.pl

Estimation of load carrying capacity on the basis of the post-buckling behaviour of thin-walled composite structures with imperfections is studied with the distortional deformations being taken into account. Our attention is focused on beams and corrugated trapezoidal plates subject to a constant bending moment or an axial compression, respectively. The structures are simply supported at the ends. The asymptotic expansion established by Byskov and Hutchinson (1977) is employed in terms of the numerical transition matrix method. The paper aims at to improving the study of the post-buckling equilibrium path of imperfect structures employing the second order non-linear approximation. The principal goal of numerical analysis is to investigate the influence of the orthotropy factor of structures upon all the buckling modes from global to local ones, and the uncoupled post-buckling state. In the solution obtained the transformation of buckling modes as the load increases up to the ultimate load and the shear-lag phenomenon are included.

Key words: thin-walled structures, composite, ultimate load

Notation

a_{111}, b_{1111}	–	coefficients appearing in the nonlinear equilibrium equations (Byskov and Hutchinson, 1977)
b_i	–	width of the ith wall of the column
$E_{ix} = E_i, E_{iy}$	–	Young moduli of the ith wall along the x and y axes, respectively
G_i	–	shear modulus of the ith wall

h_i – thickness of the ith wall of the column
k – coefficient of the reduced flexural rigidity
l – length of the column
m – number of axial half-waves of a mode
M_{ix}, M_{iy}, M_{ixy} – bending moments resultants for the ith wall
M^* – bending moment corresponding to the load carrying capacity
M_Y – plastic bending moment
$\overline{N}$ – force field
N_{ix}, N_{iy}, N_{ixy} – in-plane resultants for the ith wall
$\overline{U}$ – displacement field
u_i, v_i, w_i – displacement components of the ith wall midsurface
$\varepsilon_{ix}, \varepsilon_{iy}, \varepsilon_{ixy}$ – strain tensor components for the ith wall midsurface
η – ratio between the Young moduli in principal directions of orthotropy, $\eta = E_{iy}/E_i$
$\kappa_{ix}, \kappa_{iy}, \kappa_{ixy}$ – curvature modifications and torsion of the ith wall midsurface
λ – load parameter
λ_{cr} – value of λ at a buckling mode
ν_i, ν_{iyx} – Poisson ratio of the ith wall; the first index indicates the transverse direction and the second one shows the direction of load
σ^*_{cr} – dimensionless stress of a buckling mode, $\sigma^*_{cr} = \sigma_{cr} \cdot 10^3/E$
σ^*_s – load carrying capacity, $\sigma^*_s = \sigma_s \cdot 10^3/E$
ζ – amplitude of a buckling mode
ζ^* – imperfection amplitude corresponding to ζ

1. Introduction

Thin-walled structures (bars, beams, columns, plates and shells) made of fibrous composites find more and more frequent applied to civil engineering designs (e.g. vessels), aircraft stiffeners as well as to space vehicles.

The widespread use of fibrous composites as structural materials can be attributed to:

- High strength-to-weight and stiffness-to-weight ratios; these ratios are very important in weight-sensitive applications such as aircraft and space vehicles

- High resistance of some fibrous composites to aggressive chemical compounds and to corrosion, what can be very important in the case of vessels for some liquids and gases

- Variable thermal properties, depending on the sort of matrix and fibres (thermal insulating power, thermal conducitivity, high mechanical strength at elevated, high or very low temperatures).

In the present paper the analysis will be limited to the composites with orthotropic matrix, the fibres being evenly distributed across the structural component (plate, beam wall) along two directions perpendicular to each other but parallel to the principal directions of orthotropy of the matrix. Such an orthotropic material with a given orthotropy factor will further be dealt with on the macro-scale as a homogenous one.

A macrostructure of the composite will be characterised by its mechanical and strength properties such as moduli of elasticity along principal directions of orthotropy, Poisson ratios, shear modulus, tensile, compressive and bending strengths, etc.

In the present paper the delamination of composite materials is not taken into account. In such a case other methods of analysis should be applied.

1.1. Stability of structures made of orthotropic fibrous composites

Thin-walled composite structures may reveal many buckling modes and in some of them the structure can bear the load after local buckling. Determination of their load carrying capacity requires including imperfections into the non-linear analysis of stability.

The concept of buckling involves the general asymptotic non-linear theory of stability. The theory is based on asymptotic expansions of the post-buckling path. If the analysis of the stability problem of thin-walled structures is limited to the first order approximation only, the imperfection sensitivity can be obtained. Determination of the post-buckling equilibrium path requires the second order approximation to be taken into account.

A more comprehensive review of the literature on the coupled buckling analysis of isotropic structures can be found in the papers by Koiter and Pignataro (1976), Manevich (1988), Pignataro et al. (1985), Sridharan and Ali (1985), Sridharan and Peng (1989), Królak (1990), Kołakowski (1989, 1993).

The first study of interaction between the buckling modes in thin-walled composite structures were carried out by Godoy et al. (1995), Kołakowski and Królak (1995), Kołakowski et al. (1999), Królak and Kołakowski (1995).

Many composite structural components are subject to compression and bending causing a danger of the stability loss. Having made the above assumptions, the analysis of stability of thin-walled composite beam-columns poses no difficulties, especially if the flexural rigidity is known for the structure under consideration.

In contrast to our previous works on coupled stability of composite structures, in the present contribution the thin-walled structures are analysed, the lowest values of critical loads of which, differ substantially for various buckling modes. Therefore, the buckling modes of such structures can be considered as independent (uncoupled stability).

The main goal of this study is to determine the approximate estimation of the load carrying capacity of orthotropic fibrous composite structures for the uncoupled buckling.

In the current method (Kołakowski et al., 1999) the post-buckling behaviour of a thin-walled composite structure in the elastic range subject to an axial compression or constant bending moment is examined on the basis of Byskov and Hutchinson method (1977). The study is based on the numerical method of the transition matrix using Godunov's orthogonalization. Instead of the finite strip method, the exact transition matrix method is used in this case. The most important advantage of this method consists in the fact that it enables one to describe a complete range of behaviour of the thin-walled structures from the overall to local stability for the uncoupled buckling analysis. In the solution obtained, the co-operation between all the structure walls being taken into account, transformation of buckling modes with the increase of load, shear-lag phenomenon and effect of cross-sectional distortions are included. The distortion instability of beam-columns is investigated within the framework of non-linear theory.

2. Structural problem

Prismatic structures, of the length l, whose flat walls are treated as thin-walled homogenous orthotropic rectangular plates are considered. These rectangular plates, of the principal axes of orthotropy parallel to their edges, are connected along their longitudinal edges. The structures are simply supported at their ends.

The cross-section of a structure composed of a few plates is presented in Fig.1 along with the local Cartesian co-ordinate systems.

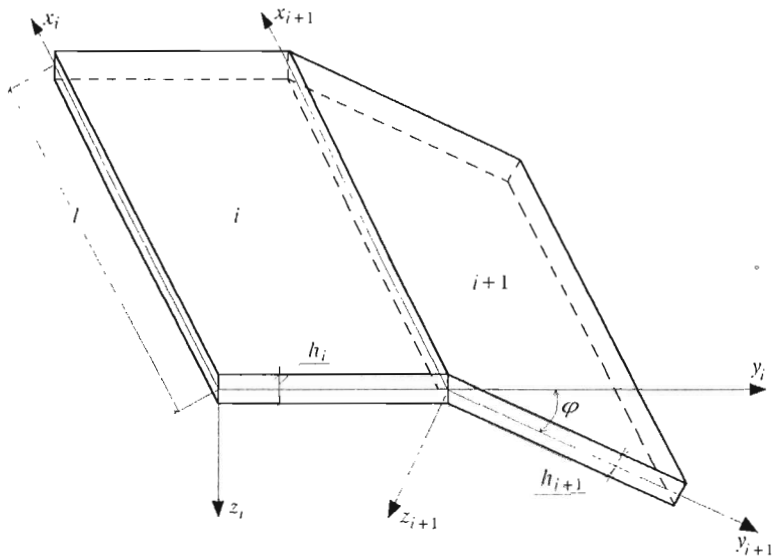

Fig. 1. Segment of a structure with the co-ordinate axes

A plate model is applied. For the ith plate component more precise geometrical relationships are assumed in order to allow for consideration of both the out-of-plane and in-plane bendings of each plate

$$\begin{aligned} \varepsilon_{ix} &= u_{i,x} + \frac{1}{2}(w_{i,x}^2 + v_{i,x}^2) & \kappa_{ix} &= -w_{i,xx} \\ \varepsilon_{iy} &= v_{i,y} + \frac{1}{2}(w_{i,y}^2 + u_{i,y}^2) & \kappa_{iy} &= -w_{i,yy} \\ 2\varepsilon_{ixy} &= \gamma_{ixy} = u_{i,y} + v_{i,x} + w_{i,x}w_{i,y} & \kappa_{ixy} &= -w_{i,xy} \end{aligned} \tag{2.1}$$

The physical relationships for the ith wall are formulated in the following way

$$\begin{aligned} N_{ix} &= \frac{E_i h_i}{1-\eta_i\nu_i^2}(\varepsilon_{ix} + \eta_i\nu_i\varepsilon_{iy}) & M_{ix} &= D_i(\kappa_{ix} + \eta_i\nu_i\kappa_{iy}) \\ N_{iy} &= \frac{E_i h_i \eta_i}{1-\eta_i\nu_i^2}(\nu_i\varepsilon_{ix} + \eta_{iy}) & M_{iy} &= \eta_i D_i(\nu_i\kappa_{ix} + \kappa_{iy}) \\ N_{ixy} &= G_i h_i \gamma_{ixy} = 2G_i h_i \varepsilon_{ixy} & M_{ixy} &= D_{1i}\kappa_{ixy} \end{aligned} \tag{2.2}$$

where

$$\eta_i = \frac{E_{iy}}{E_i} = \frac{\nu_{iyx}}{\nu_i} \tag{2.3}$$

The differential equilibrium equations resulting from the Principle of Virtual Work and corresponding to Eqs (2.1) for the ith plate can be written as follows

$$\begin{aligned} &N_{ix,x} + N_{ixy,y} + (N_{iy}u_{i,y})_{,y} = 0 \\ &N_{ixy,x} + N_{iy,y} + (N_{ix}v_{i,x})_{,x} = 0 \\ &(N_{ix}w_{i,x})_{,x} + (N_{iy}w_{i,y})_{,y} + (N_{ixy}w_{i,x})_{,y} + \\ &+(N_{ixy}w_{i,y})_{,x} + M_{ix,xx} + M_{iy,yy} + 2M_{ixy,xy} = 0 \end{aligned} \tag{2.4}$$

The solution of these equations for each plate should satisfy the kinematic and static continuity conditions at the junctions of adjacent plates and the boundary conditions referring to the free support of the structure at its both ends, i.e. $x = 0$ and $x = l$.

The non-linear problem is solved by means of the Byskov and Hutchinson asymptotic method (1977). The displacement fields $\overline{U}$, and sectional force fields $\overline{N}$, are expanded in power series in the buckling mode amplitude ζ (ζ is the amplitude of buckling mode divided by the thickness of the first component plate h_1)

$$\begin{aligned} \overline{U} &= \lambda \overline{U}_i^{(0)} + \zeta \overline{U}_i^{(1)} + \zeta^2 \overline{U}_i^{(2)} + ... \\ \overline{N} &= \lambda \overline{N}_i^{(0)} + \zeta \overline{N}_i^{(1)} + \zeta^2 \overline{N}_i^{(2)} + ... \end{aligned} \tag{2.5}$$

where

$\overline{U}_i^{(0)}, \overline{N}_i^{(0)}$ – pre-buckling fields
$\overline{U}_i^{(1)}, \overline{N}_i^{(1)}$ – buckling mode fields
$\overline{U}_i^{(2)}, \overline{N}_i^{(2)}$ – post-buckling fields.

By substituting Eqs (2.5) into the equations of equilibrium (2.4), junction conditions and boundary conditions, the boundary value problems of zero, first and second orders can be obtained. The zero approximation describes the pre-buckling state while the first approximation, that is the linear problem of stability, enables us to determine the critical loads of global and local values and their buckling modes. The second order boundary problem describes the post-buckling equilibrium path.

The non-linear equilibrium path for the uncoupled buckling mode regarding the amplitude ζ^* of buckling mode imperfection (Byskov and Hutchin-

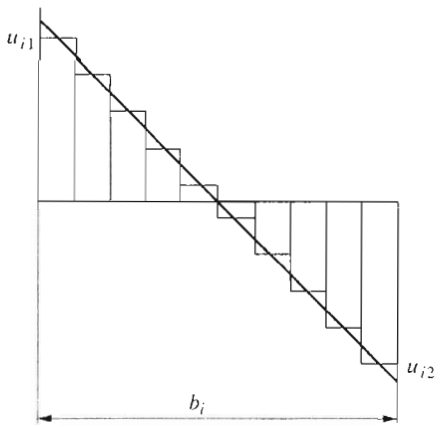

Fig. 2. Discretization of a linear distribution of longitudinal displacements by means of finite strips

son, 1977) has the following form

$$a_1\Big(1-\frac{\lambda}{\lambda_{cr}}\Big)\zeta + a_{111}\zeta^2 + b_{1111}\zeta^3 + \ldots = a_1\frac{\lambda}{\lambda_{cr}}\zeta^* \tag{2.6}$$

and the corresponding formula for the total elastic potential energy

$$V_e = -\frac{1}{2}a_0\lambda^2 + \frac{1}{2}a_1\Big(1-\frac{\lambda}{\lambda_{cr}}\Big)\zeta^2 + \frac{1}{3}a_{111}\zeta^3 + \frac{1}{4}b_{1111}\zeta^4 - a_1\frac{\lambda}{\lambda_{cr}}\zeta\zeta^* \tag{2.7}$$

where

λ – load parameter
λ_{cr} – critical value of λ
V_{e0} – energy of the pre-buckling state, $V_{e0} = a_0\lambda^2/2$

The coefficients a_0, a_1, a_{111}, b_{1111} in Eqs (2.6) and (2.7) are described in details the in papers of Byskov and Hutchinson (1977) or Królak (1990).

The post-buckling coefficient a_{111} depends only on the buckling mode whereas the coefficient b_{1111} depends also on the second order field.

The result of integration along x direction indicates that the post-buckling coefficient a_{111} equals zero when the wave number associated with the buckling mode is even, while b_{1111} coefficient is not equal to zero.

The relation between the post-buckling and the pre-buckling stiffnesses of the imperfect structures defines the coefficient of the reduced flexural rigidity (Manevich and Kołakowski, 1996)

$$k = \Big[1 + \frac{a_1\zeta\lambda_{cr}}{a_0\lambda}\Big(\frac{1}{2}\zeta + \zeta^*\Big)\Big]^{-1} \tag{2.8}$$

In a special case of the ideal structures $\zeta^* = 0$ and of the symmetrical characteristic with respect to deflections for the uncoupled buckling mode $a_{111} = 0$

$$\overline{k} = \lim_{\lambda \to \infty} k = \left(1 + \frac{a_1^2}{2a_0 b_{1111}}\right)^{-1} \tag{2.9}$$

The detailed description of the method of solution to the problem was given by Kołakowski et al. (1999).

At the point where the dimensionless load carrying capacity $\sigma_s^* = \sigma_s \cdot 10^3/E$ (instead of the load parameter λ_s) reaches its maximal value for the imperfect structure (limit points) the Jacobian of the nonlinear system of equilibrium path corresponding to (2.6) is equal to zero (for more detailed analysis see Byskov and Hutchinson (1977), Królak (1990)).

Including the displacements and loads components in the midsurface of walls within the first order approximation into consideration and using more precise geometrical relationships allowed for analysis of the shear-lag phenomenon, distortions of the cross-sections and all possible buckling modes including the mixed buckling mode (e.g. flexural-distorsional or local-distorsional one), for details see Kołakowski and Królak (1995), Kołakowski et al. (1997), Kowal-Michalska et al. (1998)).

In this paper the assumption of non-zero deflection within the second order approximation accounts for the transformation of displacement and force fields with the increase of loading that is disregarded in most works.

3. Determination of the load carrying capacity of a square orthotropic beam

The thin-walled orthotropic beam of a square cross-section is considered (Fig.3). Dimensions of the cross-section are taken after Lee et al. (1984) and Manevich and Kołakowski (1996) dealing with isotropic beams, i.e.

$$b = 100 \text{ mm} \qquad h = 1.25 \text{ mm} \qquad l = 700 \text{ mm}$$

Mechanical properties of orthotropic materials are assumed after Chandra and Raju (1973). In a general case the load carrying capacity can be determined basing on the corresponding strength (effort) criterion.

For post-buckling uncoupled analysis within the elastic range, one can obtain only an approximation of the load carrying capacity on the basis of a simplified threshold criterion.

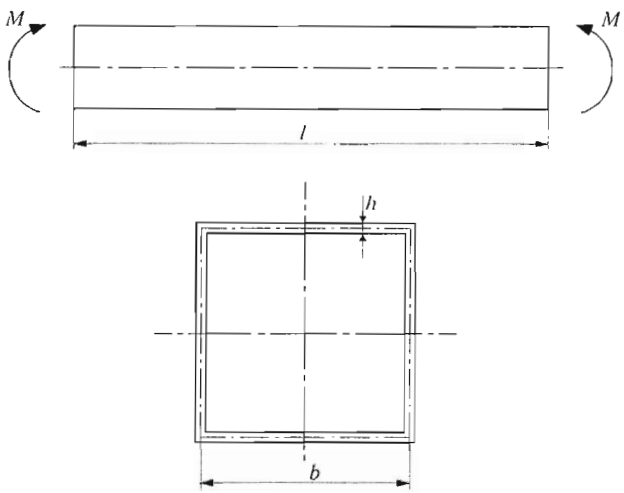

Fig. 3. Beam of a square cross-section subjected to pure bending

In this paper, the following criterion is adopted for the load carrying capacity M^*:

- In a compressed plate, the yield stress is attained at a limit-load value lower than the critical moment M_{cr}. In this case we are dealing with the pre-buckling bending, hence, it is assumed that $k = 1$, see Eq (2.8)
- In a compressed plate, the yield stress is attained at a limit moment value higher than the critical moment M_{cr}, i.e., at $k < 1$, see Eq (2.8).

However, in order to determine maximum stresses in a plate under compression, one must find not only the reduced flexural stiffness but also the position of effective neutral axis of the cross-section; this requires one of the hypotheses concerning the effective plate width be accepted. In this paper only the width of a compressed flange is reduced to obtain the real decrease in the cross-section flexural stiffness after a local buckling (cf Manevich and Kołakowski (1996), for isotropic structures). This approach provides a lower bound to the load carrying capacity.

In this paper the approximate method of the determination of load carrying capacity is presented for thin-walled orthotropic (composite) beams subject to bending.

The following assumptions have been accepted:

- Young modulus in the longitudinal direction is constant for all the considered cases $E_x = E = \text{const}$

- Young modulus in the transverse direction is variable and depends on the wall orthotropy factor η ($E_y = \eta E$), where η can vary within the range $0.0728 \leqslant \eta \leqslant 13.7362$ (see Table 1)

- Value of the yield stress in all cases is constant and less or equal to the yield stress in tension $\sigma_Y = E/1000$.

Table 1. Elastic constants for various types of the composite beam-columns

Spec. No.	η	ν	G/E
1	13.7362	0.02184	0.4065
2	7.6045	0.03945	0.4091
3	3.2992	0.09093	0.4002
4	1.9747	0.15192	0.3937
5	1.4202	0.21123	0.4009
6	1.1964	0.25074	0.3882
7	1.0000	0.3	0.3846
8	0.8358	0.3	0.3245
9	0.7041	0.3	0.2823
10	0.5064	0.3	0.1994
11	0.3031	0.3	0.1213
12	0.1315	0.3	0.0538
13	0.0728	0.3	0.0296

Three difrenet types of orthotropic beams, for $0.0728 \leqslant \eta \leqslant 13.7362$ are considered.

3.1. Type I

In the analysed case the material properties of each wall of beam are the same.

The estimation results of the load carrying capacity in the second order non-linear approximation of the asymptotic theory are presented in Fig.4. The curve M_{cr}/M_Y represents the results yielded by the linear analysis while the curve M^*/M_Y illustrates the load carrying capacity of the orthotropic beam as a function of wall orthotropy parameter η. M_Y is the value of a bending moment (calculated on the basis of the well-known formula of the strength of materials) for which the yield limit is reached in the compressed flange.

From the diagrams follows that for $3.2992 \leqslant \eta \leqslant 13.7362$ the plasticization of the compressed flange precedes the stability loss, therefore the ultimate

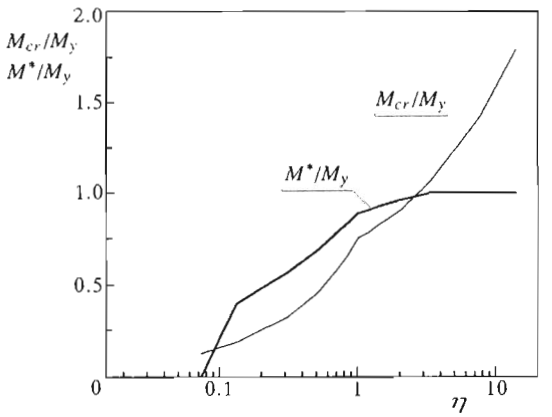

Fig. 4. Load carrying capacity for the beam of type I

bending moment is equal to the moment corresponding to the plastic moment $M^*/M_Y = 1$.

For values of the orthotropy parameter $0.0728 \leqslant \eta \leqslant 3.2992$ the buckling occurs in the elastic range. The beam can bear loading in the post-buckling state and its load carrying capacity is higher than the critical load, i.e. $M^*/M_{cr} > 1$.

With the loading growth the effective cross-section area of the compressed flange decreases.

When calculating the effective cross-section it was assumed that only the width of the compressed flange is reduced. For the orthotropy parameter $\eta = 0.0728$ the above assumption makes no sense and the widths of the webs (subject to bending) should also be reduced – which was not the subject matter of the study. Thus, in Fig.4 there are no results for this value of η.

From the presented diagrams it can be seen that with the increasing value of the orthotropy parameter η (and the increasing value of Young modulus in the transverse direction E_y) the load carrying capacity of a beam increases.

For the isotropic material $\eta = 1$ and $\sigma_Y = 191.3\,\mathrm{MPa}$ the value of M^*/M_Y, obtained in the present work, equals 0.893 while that emerging from the FEM (Lee et al., 1984) was $M^*/M_Y = 0.93$.

It should be also remembered that the analysis presented here deals with dimensionless parameters, however, that dimensional critical stresses change proportionally to the modulus E because $\sigma_{cr} = \sigma^*_{cr}E/1000$ and $M^*_{cr} = 2\sigma^*_{cr}I/b_2$, where I is the cross-section moment of inertia.

A designer should choose properly the Young moduli E and E_y for

materials almost isotropic. Taking mean values into account may result in a wrong estimation of the load carrying capacity of the structure.

The adoption of the plate model for the beam-column allowed us to take into account the effect of the parameter η (modulus E_y) on the critical values of global and local buckling stresses that would not be possible if a beam-bar model was applied.

For the analysed beam and for the assumed range of the orthotropy factor $0.0728 < \eta \leqslant 3.2992$ the averaged obtained value of the limit coefficient of the reduced flexural rigidity is $\overline{k} = 0.736$, while the minimal and maximal values are, respectively: $\overline{k}_{\min} = 0.719$, $\overline{k}_{\max} = 0.749$. It allows us to conclude that the presented method of the estimation of the load carrying capacity of orthotropic structures should describe, with a satisfactory accuracy, the lower bound of the load carrying capacity estimation in real structures.

The semi-analytical method for the lower bound estimation of coefficient $\overline{k}$ within the framework of first order approximation (Kołakowski, 1996) also yields an almost constant value within the considered range of η ($\overline{k} = 0.67$).

In Table 2 the values of post-buckling coefficients $\overline{b}_{1111}$ and $\overline{b}^{*}_{1111}$ are presented for the considered range of orthotropy factor: within the second order approximation (2.6) (for more detailed analysis see Kołakowski et al. (1999)) $\overline{b}_{1111} = b_{1111}/a_1$, within the first order approximation (Kołakowski, 1996) $\overline{b}^{*}_{1111} = b_{1111}/a_1$.

Table 2. Values of the post-buckling coefficients

Spec. No.	η	$\overline{b}^{*}_{1111}$	$\overline{b}_{1111}$	$\left(\frac{\overline{b}^{*}_{1111}}{\overline{b}_{1111}} - 1\right) \cdot 100\%$
		1	2	3
1	13.7362	0.62	0.51	22%
2	7.6045	0.60	0.50	20%
3	3.2992	0.49	0.44	11%
4	1.9747	0.48	0.43	12%
5	1.4202	0.42	0.39	8%
6	1.1964	0.45	0.41	10%
7	1.0000	0.37	0.35	3%
8	0.8358	0.42	0.39	8%
9	0.7041	0.48	0.44	9%
10	0.5064	0.46	0.43	7%
11	0.3031	0.48	0.44	9%
12	0.1315	0.58	0.51	14%
13	0.0728	0.53	0.46	15%

The maximal difference (22%) occurs for $\eta = 0.0728$. It can be seen that a satisfactory agreement between the post-buckling coefficients is achieved.

Estimation of the values of the coefficient $\bar{b}^*_{1111}$ within the framework of first order approximation (for $0.3031 \leqslant \eta \leqslant 3.2992$, and differences about 10%) allows one to avoid numerical problems posed by the second order approximation. It allows for a quantitative analysis of the coupled buckling and determination of the load carrying capacity.

3.2. Type II

In this case the webs (lateral walls) of the orthotropic beam and the bottom flange (subject to tension) are made of a material of the following properties (Table 1):

$$\eta = 0.0728 \qquad \nu = 0.3 \qquad G/E = 0.0296$$

It is assumed that the compressed (upper) flange is made from a material revealing different values of orthotropy factor η (Table 1).

The results obtained for a beam of this type are presented in Fig.5. For the values of orthotropy factor $\eta \leqslant 0.3031$ widths of the webs subject to bending should also be reduced, as for type I. Thus in Fig.5 the results of calculations for these values of η are not presented.

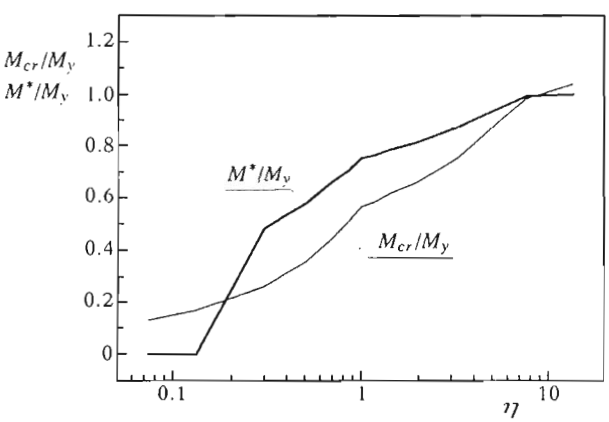

Fig. 5. Load carrying capacity for the beam of type II

Comparing the results presented in Fig.4 and Fig.5 it can be noticed that for type II both the value of the critical load M_{cr} and the value of the load carrying capacity M^* are lower than for type I.

Within the range of the orthotropy factor $0.3031 \leqslant \eta \leqslant 7.604$ the load carrying capacity of beam II is lower up to 15% in comparison with beam I.

3.3. Type III

In the third analysed case of the orthotropic beam it is assumed that the bottom part of beam lying below the neutral axis of bending (the bottom flange and the part of webs below the midplane) (Fig.3) is made of a material of the following properties:

$$\eta = 0.0728 \qquad \nu = 0.3 \qquad G/E = 0.0296$$

The upper part of beam, i.e. the compressed (upper) flange and the part of webs above the neutral axis of bending are made of a material revealing different values of the orthotropy factor η (Table 1).

The results presented in Fig.6 are almost identical with the results obtained for beam I.

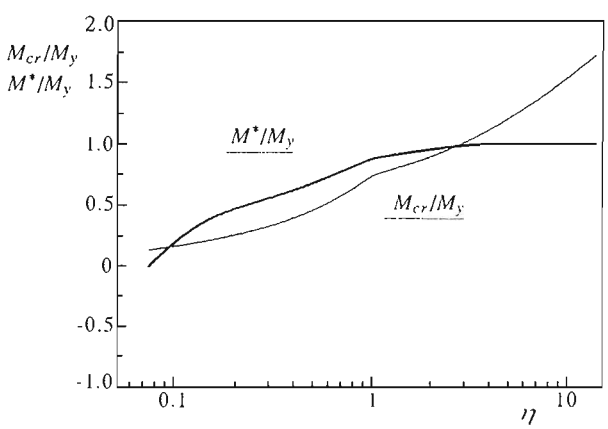

Fig. 6. Load carrying capacity for the beam of type III

It allows one to conclude that the stability and load carrying capacity of the orthotropic beam is determined by properties of the parts of a structure that are subject to compression.

For the above assumptions about the beam design the technological reasons may decide of a realisation of type I or type III.

4. Load carrying capacity for corrugated trapezoidal plate

Stiffeners are widely used in many types of metal structures. These stiffeners carry a portion of loading and subdivide the plate element into smaller sub-elements, thus increase considerably the load-carrying capacity. The shape, size and position of stiffeners in thin-walled structures exerts a strong influence on the stability and post-buckling behaviour of the thin-walled structures. The minimum rigidity of intermediate stiffeners necessary for limiting the buckling to the plate elements was studied; e.g., by Konig (1978), Teter et al. (1996).

A trapezoidal shape of a segment increases significantly the flexural rigidity of a plate, improving therefore, its load carrying capacity.

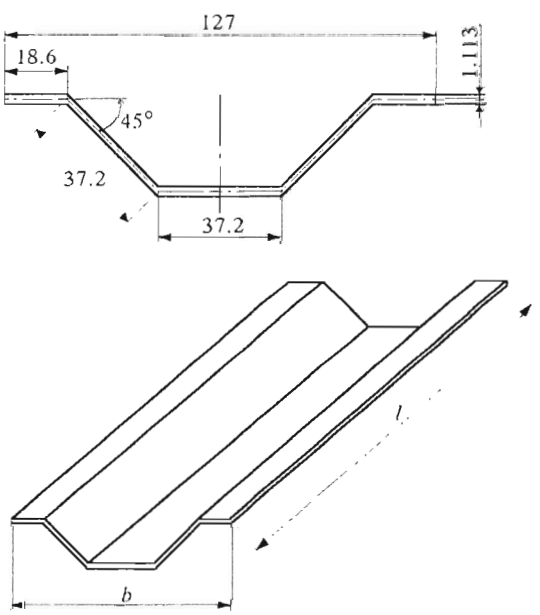

Fig. 7. A segment of a corrugated trapezoidal plate

The detailed calculations are presented for an infinitely wide corrugated trapezoidal plate of length l, subject to compression. The loaded edges of plate are simply supported. The analysis of such a segment is sufficient in the case of trapezoidal plate with a large number of segments (Fig.7), when the boundary conditions may be neglected in the analysis. The following dimensions of an individual corrugated segment of a trapezoidal plate are assumed – the so-

called NASA plate (Dawe and Wang, 1994):

$$l = 762 \text{ mm} \qquad h = 1.113 \text{ mm} \qquad b = 127 \text{ mm}$$

The mechanical properties of orthotropic materials are assumed as in the previous analysis (Table 1).

The plate model is applied to all walls of the segment.

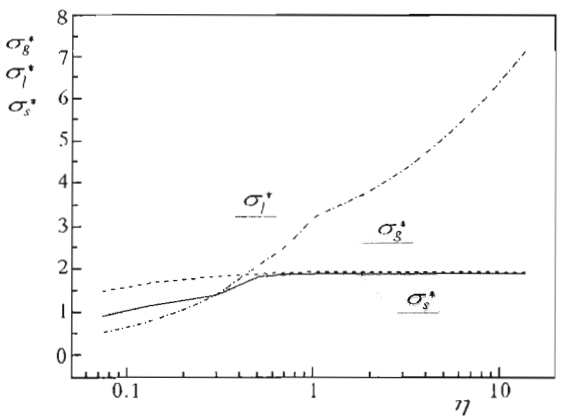

Fig. 8. Dimensionless critical stresses versus orthotropy parameter η

In Fig.8 the calculated results of two lowest values of the critical stresses σ^*_{cr} are presented for the considered range of orthotropy parameter. The segment buckling in a form of one half-wavelength $m = 1$ in the longitudinal direction corresponds to the global buckling of such a segment (for more detailed analysis the Reader is referred to Manevich (1988), Kołakowski (1989)). A larger number of half-waves $m > 1$ corresponds to the local buckling. It should be emphasized that the value of global critical stress σ^*_g determines also the load carrying capacity.

In the case of isotropic segment the critical stresses are:

global buckling $m = 1$ $\qquad \sigma^*_g = 1.92$
local buckling $m = 20$ $\qquad \sigma^*_l = 3.24$

In the linear analysis of the NASA plate with a square contour (Dawe and Wang, 1994), i.e. composed of six segments and simply supported along all edges, the values of critical stresses equal:

global buckling $m = 1$ $\qquad \sigma^*_{cr} = \sigma^*_g = 2.02$
local buckling $m = 18$ $\qquad \sigma^*_{cr} = \sigma^*_l = 3.30$

When taking into account one segment only, it can be seen that no substantial differences between the values of critical stresses for both the buckling modes appear.

The local buckling is more sensitive to variation of the orthotropy factor than to the global buckling.

It can be clearly seen from Fig.8 that in the range of the orthotropy parameter $0.4 \leqslant \eta \leqslant 13.7362$ the value of global buckling load is lower than the local one so the global load is the ultimate load. The analysis of coupled stability has shown that the interaction between global buckling mode and local ones is rather small and practically can be neglected in the non-linear analysis of the segment. The decrease in critical load did not exceed 3%.

For $\eta \leqslant 0.4$ the local critical load is lower than the global one and the segment can bear loading in the post-buckling state for moderate initial imperfections. It seems that putting into practice such NASA plates (for $\eta \leqslant 0.4$) is not much justified from the economic point of view. Thus it can be assumed that the local critical load is also the ultimate load.

In Fig.8 the ultimate load σ_s^* determined within the framework of second order coupled stability analysis (Kołakowski et al., 1999) is also shown. For the structures with imperfections $|\zeta_g^*| = 1.0$, $|\zeta_l^*| = 0.2$ and for $\eta \geqslant 0.5064$ the value of load carrying capacity σ_s^* is smaller than the value of global critical stress σ_g^* (for more detailed analysis see Kołakowski et al. (1999)) while for $\eta \leqslant 0.3034$ and $\sigma_l^* < \sigma_g^*$, the value of σ_s^* is greater than the value of σ_l^* prescribed by the theory and experiments.

5. Conclusions

The analysis carried out proves that for the considered range of orthotropy factor η it is possible to estimate, with the accuracy sufficient for engineering purposes, the lower bound of the load carrying capacity using linear analysis of stability (first order approximation of the Byskov-Hutchinson theory).

The applied method describing the buckling of thin-walled structures from global to local stability loss can be easily implemented into a computer-aided system (CAD/CAM).

The present paper deals with the analysis of influence of the wall orthotropy factor upon the uncoupled elastic buckling of thin-walled orthotropic structures subject to compression or bending.

Numerical calculations prove that in the case of orthotropic structures distinct differences may occur if a plate model or a beam-bar model of a column

is assumed. It is obvious when the deplanation of cross-section is considered, which implies the distorsional buckling to be taken into account.

Acknowledgements

The work was supported by the State Committee for Scientific Research (KBN) under grant No. PB 251/T07/97/12.

References

1. BYSKOV E., HUTCHINSON J.W., 1977, Mode Interaction in Axially Stiffened Cylindrical Shells, *AIAA J.*, **15**, 7, 941-948
2. CHANDRA R., RAJU B.B., 1973, Postbuckling Analysis of Rectangular Ortothropic Plates, *Int. J. Mech. Sci.*, **16**, 81-89
3. DAWE D.J., WANG S., 1994, Buckling of Composite Plates and Plate Structures Using the Spline Finite Strip Method, *Composites Engineering*, **4**, 11, 1099-1117
4. GODOY L.A., BARBERO E.J., RAFTOYIANNIS I., 1995, Interactive Buckling Analysis of Fiber-Reinforced Thin-Walled Columns, *Int. J. Composite Structures*, **29**, 5, 591-623
5. KOITER W.T., PIGNATARO M., 1976, An Alternative Approach to the Interaction Between Local and Overall Buckling in Stiffened Panels; In: *Buckling of Structures – Proc. of IUTAM Symposium, Cambridge, 1974*, 133-148
6. KOŁAKOWSKI Z., 1989, Mode Interaction in Wide Plate with Angle Section Longitudinal Stiffeners Under Compression, *Engineering Transactions*, **37**, 1, 117-135
7. KOŁAKOWSKI Z., 1993, Influence of Modification of Boundary Conditions on Load Carrying Capacity in Thin-Walled Columns in the Second Order Approximation, *Int. J. Solids Structures*, **30**, 19, 2597-2609
8. KOŁAKOWSKI Z., 1996, A Semi-Analytical Method for the Analysis of the Interactive Buckling of Thin-Walled Elastic Structures in the Second Order Approximation, *Int. J. Solids Structures*, **33**, 22, 3779-3790
9. KOŁAKOWSKI Z., KOWAL-MICHALSKA K., KĘDZIORA S., 1997, Determination of Inelastic Stability of Thin-Walled Isotropic Columns Using Elastic Orthotropic Plate Equations, *Mechanics and Mechanical Engineering*, **1**, 1, 79-100
10. KOŁAKOWSKI Z., KRÓLAK M., 1995, Interactive Elastic Buckling of Thin-Walled Closed Orthotropic Beam-Columns, *Engineering Transactions*, **43**, 4, 571-590

11. KOŁAKOWSKI Z., KRÓLAK M., KOWAL-MICHALSKA K., 1999, Modal Interactive Buckling of Thin-Walled Composite Beam-Columns Regarding Distortional Deformations, *Int. J. Eng. Sci.*, (to be published)

12. KONIG L., 1978, Transversely Loaded Thin-Walled C-Shaped Panels with Intermediate Stiffeners. Document D7: Swedish Council for Building Research, Sweden

13. KOWAL-MICHALSKA K., KOŁAKOWSKI Z., KĘDZIORA S., 1998, Global and Local Inelastic Buckling of Thin-Walled Orthotropic Columns by Elastic Asymptotic Solutions, *Mechanics and Mechanical Engineering*, **2**, 2, 209-232

14. KRÓLAK M. (edit.), 1990, *Post-Buckling Behaviour and Load Carrying Capacity of Thin-Walled Plate Girders*, PWN Warsaw-Łódź, (in Polish)

15. KRÓLAK M., KOŁAKOWSKI Z., 1995, Interactive Elastic Buckling of Thin-Walled Open Orthotropic Beam-Columns, *Engineering Transactions*, **43**, 4, 591-602

16. LEE H.P., HARRIS P.J., CHENG-TZU THOMAS HSU, 1984, A Nonlinear Finite Element Computer Program for Thin-Walled Members, *Thin-Walled Structures*, **2**, 355-376

17. MANEVICH A.I., 1988, Interactive Buckling of Stiffened Plate under Compression, *Mekhanika Tverdogo Tela*, **5**, 152-159 (in Russian)

18. MANEVICH A.I., KOŁAKOWSKI Z., 1996, Influence of Local Postbuckling Behaviour on Bending of Thin-Walled Beams, *Thin-Walled Structures*, **25**, 3, 219-230

19. PIGNATARO M., LUONGO A., RIZZI N., 1985, On the Effect of the Local Overall Interaction on the Postbuckling of Uniformly Compressed Channels, *Thin-Walled Structures*, **3**, 283-321

20. PIGNATARO M., LUONGO A., 1987, Asymmetric Interactive Buckling of Thin-Walled Columns with Initial Imperfection, *Thin-Walled Structures*, **3**, 365-386

21. SRIDHARAN S., ALI M.A., 1985, Interactive Buckling in Thin-Walled Beam-Columns, *J. Engng. Mech. ASCE*, **111**, 12, 1470-1486

22. SRIDHARAN S., PENG M.H., 1989, Performance of Axially Compressed Stiffened Panels, *Int. J. Solids and Structures*, **25**, 8, 879-899

23. TETER A., KOŁAKOWSKI Z., 1996, Interactive Buckling of Thin-Walled Open Elastic Beam-Columns with Intermediate Stiffeners, *Int. J. Solids Structures*, **33**, 3, 315-330

Oszacowanie nośności granicznej cienkościennych konstrukcji kompozytowych

Streszczenie

W pracy przedstawiono oszacowanie nośności granicznej w oparciu o praktyczne zachowanie się cienkościennych konstrukcji z imperfekcjami przy uwzględnieniu dystorsji przekroju poprzecznego. Rozważania przeprowadzono dla belek oraz trapezowych płyt falistych obciążonych, odpowiednio, momentem gnącym i ściskaniem. Założono swobodne podparcie konstrukcji na obu końcach. Zastosowano asymptotyczną metodę Byskova i Hutchinsona (1977) przy wykorzystaniu numerycznej metody macierzy przejścia. Celem pracy jest uściślona analiza pokrytycznych ścieżek równowagi z niedokładnościami w ramach drugiego rzędu przybliżenia. Główną uwagę w obliczeniach numerycznych skoncentrowano na wpływie współczynnika ortotropii konstrukcji na wszystkie postacie wyboczenia od globalnego do lokalnego i niesprężony stan powyboczeniowy. W rozważaniach uwzględniono transformację postaci wyboczenia ze wzrostem obciążenia aż do nośności granicznej i zjawisko "shear-lag".

Manuscript received March 4, 1999; accepted for print October 11, 1999